



NET PROTON AND CHARGED MESON FLOW IN RELATIVISTIC HEAVY ION COLLISIONS AT 200 GEV/A.

Majhar Ali

Kalindi College, University of Delhi, New Delhi, Delhi, India

A statistical thermal model for the hot and dense hadronic matter produced in the ultra-relativistic central collisions of heavy nuclei is used. The matter formed is assumed to be consisting of regions moving with increasing rapidity (y_{FB}) along the rapidity axis. A Gaussian profile in y_{FB} is used to weigh the contributions of these regions to the final state emitted hadron's population. A quadratic profile in y_{FB} is used to fix the baryon chemical potentials of these regions.

This situation is found to emerge from the nuclear transparency effect in those collisions at such ultra-relativistic energies. We find that it is possible to explain not only the net proton, and \bar{p}/p ion flow but also the individual proton, antiproton, Kaon, antiKaon. It is interesting to find that the model can successfully explain the strange sector data also quite well, measured in the same experiment by the BRAHMS collaboration. This is achieved by using single set of the model parameters.

1. Introduction

The yields of baryons and antibaryons are an important indicator of the multi-particle production phenomenon in the ultra-relativistic nucleus-nucleus collisions. Great amount of experimental data have been obtained in such experiments ranging from the AGS energies to the RHIC. The

study of ultra-relativistic nuclear collisions allows us to learn how baryon numbers, initially carried by the nucleons, are distributed in the final state [1]. It is possible to obtain important information about the energy loss of the colliding nuclei by analyzing the rapidity dependence of the p and \bar{p} production. The measurement of the *net* proton flow (i.e. $p - \bar{p}$) in such experiments can throw light on the collision scenario, viz. the extent of nuclear stopping/transparency, formation of the fireball(s) and the degree of thermo-chemical equilibration of various hadronic resonances, which can be estimated by their contributions to the lighter hadrons viz. p , \bar{p} , K etc. via their decay. The net proton flow at the AGS energy showed a peak at midrapidity, while at the top SPS energy ($\sqrt{s_{NN}} \approx 17.3$ GeV) the distribution started showing a minimum at midrapidity. The SPS data at different energies (20, 30, 40, 80, 158 GeV/A) show [1] that at midrapidity the p yield decreases gradually with increasing energy in contrast to the rising \bar{p} yield. This implies that at SPS energies the nuclear collisions start exhibiting some transparency. Hence this new property namely the extended longitudinal scaling in the rapidity distributions has emerged [2 - 5]. This has been observed in pp collisions at the highest RHIC energies as well as ultra-relativistic nuclear collisions [5, 6]. Data from the BRAHMS collaboration [7] clearly show that the antiproton to proton ratio shows a maximum at mid rapidity and gradually decreases towards larger rapidities, whereas the net proton flow shows a broad minimum, spanning about ± 1 unit around mid-rapidity region of dN/dy spectra. It was therefore conjectured [7] that at RHIC energies the collisions are (at least partially) transparent. Though the midrapidity region at RHIC is not yet totally baryon free however a transition from a baryon dominated system at lower energies to an *almost* baryon free system in the midrapidity at RHIC can be observed. An interesting analysis by Stiles and Murray [2, 8] shows that the data obtained by the BRAHMS collaboration at 200 GeV/A has a clear dependence of the baryon chemical potential on rapidity which is revealed through the changing \bar{p}/p ratio with rapidity. Biedroń and Broniowski [2, 9] have done an analysis of rapidity dependence of the \bar{p}/p , K^+/K^- , π^+/π^- ratios based on a single freeze-out model of relativistic nuclear collisions. They have used a single fireball model where the baryon chemical potential depends on the spatial rapidity $\alpha_{//} = \text{arctanh}(z/t)$ inside the fireball. They use single temperature parameter for the entire fireball at the freeze-out (≈ 165 MeV). Their model is very successful in

explaining the proton, antiproton and the (Anti) Kaon rapidity spectra. They have used a parameterization for the functional dependence of the chemical potentials at low values of $|\alpha_{//}|$ as $\mu = \mu(0)[1 + A \alpha_{//}^{2.4}]$. Here the power is chosen to be 2.4 which according to these authors works better than 2. Fu-Hu Liu *et al.* have [10] attempted to describe the transverse momentum spectrum and rapidity distribution of net protons produced in such high energy nuclear collisions by using a new approach viz. a two cylinder model [11 - 13].

2. The Model

In order to describe the rapidity distribution of the produced hadrons in ultra-relativistic nuclear collisions the statistical thermal model has been extended to allow for the chemical potential and temperature to become *rapidity dependent* [5, 9, 14 - 16]. Becattini *et al.* and Cleymans *et al.* [2,5, 14 - 16] have attempted to describe the *net* proton flow data obtained at RHIC in Au – Au collisions at 200 GeV/A.

$$\frac{dN^j(y)}{dy} = A \int_{-\infty}^{+\infty} \rho(y_{FB}) \frac{dN_1^j(y - y_{FB})}{dy} dy_{FB} \quad (1)$$

Where y is the particles rapidity in the *rest frame* of the colliding nuclei and A is the overall normalization factor, which may be particle dependent. The distribution $\frac{dN^j(y)}{dy}$ represents total contributions of all the fireballs to the j^{th} hadron specie's rapidity spectra. According to the thermal model the rapidity spectra of the baryons in the individual fireball, i.e. $\frac{dN_1^j}{dy}$ can be written as:

$$\frac{dN_1^j}{dy} = 2\pi g \lambda^j \left[m_o^2 T + \frac{2m_o T^2}{\text{Cosh}y} + \frac{2T^3}{\text{Cosh}^2 y} \right] e^{-\beta m_o \text{Cosh}y} \quad (2)$$

Where T is the thermal temperature of the fireball. The m_o and λ^j are the rest mass and the fugacity of the j^{th} hadronic specie, respectively

$$\frac{d^3 n^{decay}}{d^3 p} = \left(\frac{1}{2pE} \right) \left(\frac{m_h}{p^*} \right) \int_{E_-}^{E_+} dE_h E_h \left(\frac{d^3 n_h}{d^3 p_h} \right) \quad (3)$$

Where P and E are the momentum and total energy of the product hadron and the subscript “ h ” denotes the decaying (parent) hadron. Here the contribution of the respective fireballs to the hadronic yield is not assumed to be in the equal proportions. It is rather assumed to follow a Gaussian distribution in the variable y_{FB} , centred at zero fireball rapidity ($y_{FB}=0$).

$$\rho(y_{FB}) = \frac{1}{\sqrt{2\pi}\sigma} \exp\left(\frac{-y_{FB}^2}{2\sigma^2}\right) \quad (4)$$

The value of σ determines the width of the Gaussian distribution. The experimental data provide a strong evidence that the baryon chemical potential (μ_B) of the successive fireballs should be dependent on the fireball’s rapidity (y_{FB}). A quadratic type dependence is considered [2, 4] so as to make the chemical potential (μ_B) invariant under the transformation $y_{FB} \rightarrow -y_{FB}$:

$$\mu_B = a + b y_{FB}^2 \quad (5)$$

In the recent works it has been further assumed that the temperature of the successive fireballs along the rapidity axis *decreases* (as the baryon chemical potential increases) according to a chosen parameterization [5, 17]:

$$T = 0.166 - 0.139 \mu_B^2 - 0.053 \mu_B^4 \quad (6)$$

where the units are in GeV. Here the temperature of the mid-rapidity fireball ($y_{FB} \sim 0$) is fixed at ~ 165 MeV.

3. Result and Discussion

In figures (1) and (2) we have shown the experimental dN/dy data (by the red solid circles) for the protons and antiprotons, respectively, obtained from the top 5% most central collisions at $\sqrt{s_{NN}} = 200$ GeV in the BRAHMS experiment. The errors are both statistical and systematic. The proton’s and antiproton’s dN/dy show a maximum at midrapidity and decrease towards higher rapidities ($y \sim 3$). We have fitted both the spectral shapes simultaneously for $a = 21.0$, $b = 11.2$, $\sigma = 2.1$ and T

= 175.0 MeV. We find that the theoretical curves fit the data quite well in both the cases. The experimental data have been symmetrized for the negative values of rapidity [7].

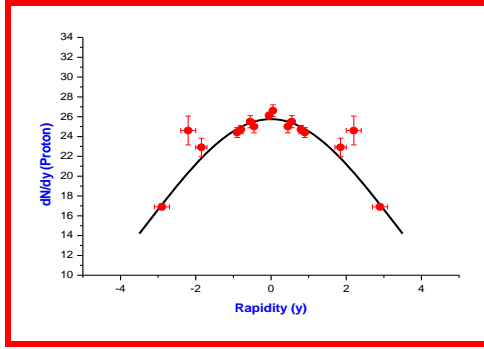


Figure (1): Proton rapidity spectra.

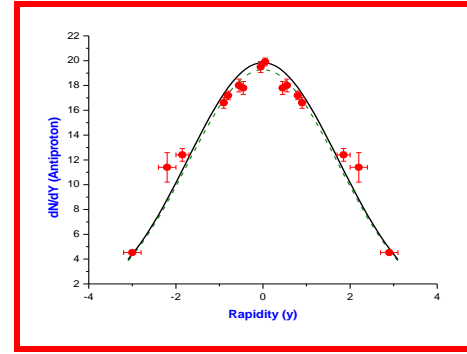


Figure (2): Antiproton rapidity spectra.

Theoretical result is shown by the solid curve.

It may be noted that the proton spectra in the figure (1) is seen to be slightly broader than the antiproton spectra in figure (2). This according to the present model seems to emerge from the fact that the baryon chemical potential $\mu_B \sim y_{FB}^2$ and the rapidity axis is assumed to be populated by the fireballs of successively increasing rapidity y_{FB} and hence increasing chemical potentials. Consequently the low rapidity (y) baryons (which have a larger population in a baryon rich fireball in thermo-chemical equilibrium) emitted in the forward (or backward) direction from a *fast* region (or fireballs with large y_{FB}), appear with a large value of rapidity (y) in the *rest frame of the colliding nuclei*. In other words as the baryon chemical potentials (μ_B) increase monotonically along the rapidity axis (as $\sim y_{FB}^2$) there is an increase in the *density* of the protons and a simultaneous suppression in the *density* of antiprotons thereby making the proton rapidity spectrum broader than that of the antiproton's. The value of the minimum X^2/DoF for the fitted curves is also sensitively dependent on the overall normalization factor A (in eqn. (1)). In Fig. (1) where we show the proton spectrum, the value of the normalization factor A = **68.36** gives a minimum $X^2/DoF = 2.996$. However, if we use the same value of normalization factor for the antiproton data in figure (2) we find that the fit is somewhat poor and we get $X^2/DoF = 6.817$, which appears to be large. Hence we applied the criteria of minimum X^2/DoF for the antiproton data independently and arrived at a slightly different (lesser) normalization factor of **66.40**, which is about 97.13 % of the proton's normalization factor. One reasonable interpretation for the lesser

value of the normalization factor for the antiprotons could be that the antiproton phase space may be approximately 97 % saturated, considering the proton's phase space to be fully chemically saturated.

Similarly this effect is also reflected in the rapidity spectra dN/dy for the net proton flow, i.e. $p - \bar{p}$ in figure (3). Here we find that by using the proton's normalization factor for both (i.e. 68.36 for p and \bar{p}) we get a fit with a value of $\chi^2/\text{DoF} = 1.527$ (dashed curve) while using the antiproton's normalization factor for both (i.e. 66.40 for p and \bar{p}) a still poorer fit is obtained with $\chi^2/\text{DoF} = 2.806$ (dashed-dotted curve). In contrast when we use the proton's and antiproton's *individual* normalization factors (i.e. 68.36 for p and 66.40 for \bar{p}) we find a much better fit with a $\chi^2/\text{DoF} = 0.554$. This is shown in figure (4) by a solid curve.

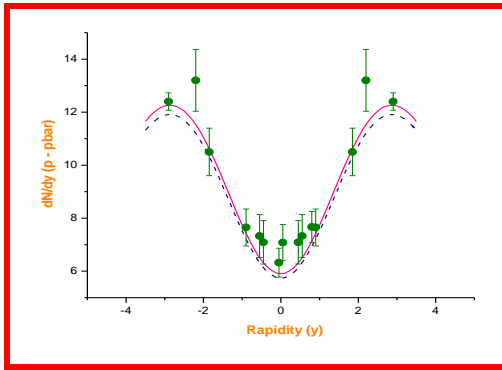


Figure (3): Rapidity spectra of the net proton flow.

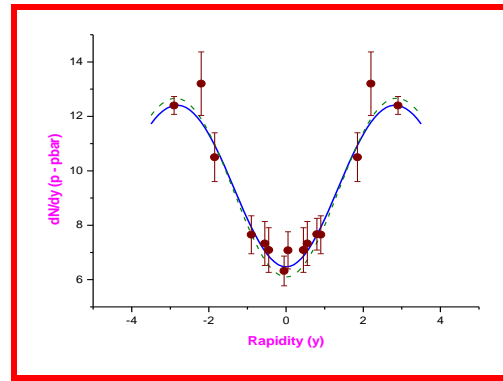


Figure (4): Rapidity spectra of the net proton flow.

Interestingly if we try to obtain the value of the normalization factor A by *independently fitting* the $p - \bar{p}$ data (whereby treating A as a free parameter) we get a minimum $\chi^2/\text{DoF} = 1.016$ for $A = 70.6$ (dashed curve). But even this fit is poorer than the one obtained by selecting the proton and antiproton's individual normalization factors i.e. 68.36 and 66.40, respectively. The experimental net proton flow distribution data shows a somewhat broad minimum around the mid-rapidity region which is well described by the theoretical solid curve in figure (4).

This experimental situation is however not as was earlier expected widely [18] that the rapidity distribution of baryons produced in the ultra-relativistic nuclear collisions will exhibit a very flat

and broad minimum, measuring several units of rapidity, centered at midrapidity. So far it has not been observed, either in the SPS experiments or even at the highest RHIC energy. The future LHC experiments may throw more light on this aspect and provide a better understanding of the nuclear transparency effect in the ultra-relativistic nuclear collisions. The present RHIC experiments at 200 GeV/A have given an indication that these nuclear collisions have begun to show at least partial transparency.

In figure (5) we have shown the rapidity spectra of the \bar{p}/p ratio. The ratio has somewhat a broad maximum (~ 0.75) in the midrapidity region which then decreases to about 25% at around $y \sim 3$.

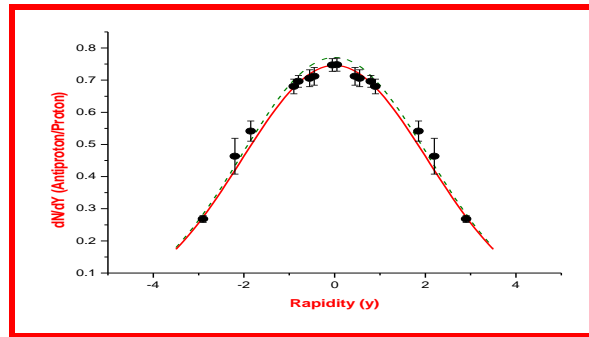


Figure (5): Rapidity spectra of \bar{p}/p ratio.

For the case of \bar{p}/p distribution when we use common normalization factors for p and \bar{p} we get a fit with a value of $X^2/\text{DoF} = 2.332$ (dashed curve). And again using their individual normalization factors (i.e. 68.36 for p and 66.40 for \bar{p}), we obtain a better fit for \bar{p}/p with $X^2/\text{DoF} = 0.854$ shown by solid curve. In other words the overall multiplying factor (or the *effective* normalization factor for this ratio) becomes 0.971 (or 97.1 %). These values are interestingly *almost* same as the one obtained from the minimum X^2/DoF criteria, by fitting the data independently. For which we find $A = 0.968$ (or 96.8 %) and minimum $X^2/\text{DoF} = 0.838$. This gives a strong support to the argument stated above also that the antiproton phase space might not be fully chemically equilibrated. This could be due to large threshold energy required for their production.

Apart from the analysis of the rapidity spectra of non-strange baryons we have also analyzed the strange meson data as measured by the BRAHMS collaboration in the top 5% most central collisions at 200 GeV/A in the same Au - Au collision experiments. We have found that in the

above model it is possible to fully account for the rapidity distribution of Kaons and AntiKaons also.

In figure (6) we have shown the rapidity spectra of Kaon flow. These data have been corrected by the BRAHMS for all the possible feed-down contributions from the heavier resonances e.g. K^* etc. The theoretical curve which fits the data is for the *same* values of the model parameters as used for the theoretical curves in figures (1) and (2). We find that the theoretical curve provides a very good fit to the data. In figure (7) we have shown the rapidity spectra of AntiKaons. Like Kaon data the anti-Kaon data is also corrected for all the possible feed-down contributions of the heavier resonances. The theoretical curve which fits the data is again for the same values of the model parameters used in figures (1) and (2). The normalization factors for both these cases obtained by fitting their individual rapidity spectra by applying the minimum χ^2/DoF criteria are almost same.

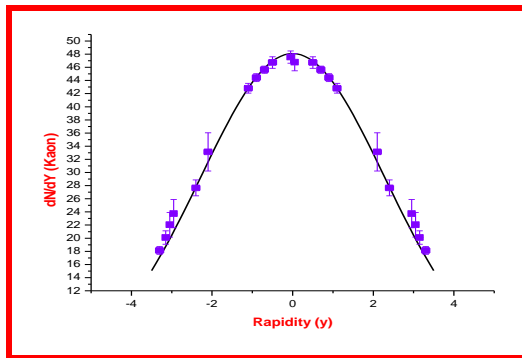


Figure (6): Rapidity spectra of Kaon flow.

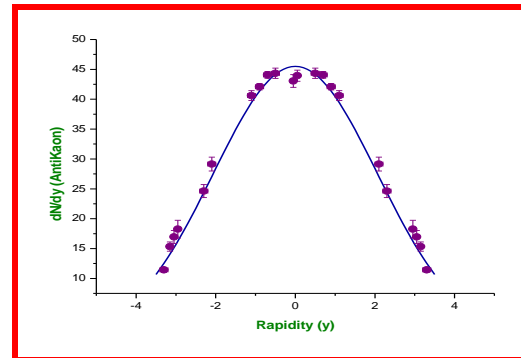


Figure (7): Rapidity spectra of Anti-Kaon flow.

We find that for Kaons $A = 45.43$ with gives minimum $\chi^2/\text{DoF} = 1.982$, while for the antiKaons we get $A = 45.8$ with minimum $\chi^2/\text{DoF} = 5.880$. Using the same normalization factor for the antiKaons as the one used for the Kaons (i.e. 45.43) we get the value of $\chi^2/\text{DoF} = 6.194$. Here the values of the normalization factors are almost same. This may be due to almost same threshold energy for the production of Kaons and antiKaons. Since these are copiously produces through the reactions like $\pi\pi \rightarrow K \bar{K}$.

Here again we find that the Kaon spectra is broader than the AntiKaon spectra as is also noticed for the proton spectra which is broader than the antiproton spectra. This is again due to the increasing chemical potential of the successive fireballs along the rapidity axis.

The mid-rapidity data (for $|y| < 1$) available from STAR [19] fit quite well in both these cases. The theoretical curves are for the same values of the model parameters as the ones used for protons, antiprotons, Kaons and antiKaons.

In figure (8) we have shown the theoretical fit to the pion's experimental data. The pion data has been corrected for all the possible feed-down contributions from the heavier resonances by the BRAHMS. The pion spectrum is also fitted for the same values of the model parameters as used for p , \bar{p} , and K , \bar{K} . The pion rapidity spectrum is sensitive only to the two model parameters, which are T and σ . The values of \mathbf{a} and \mathbf{b} have no role to play whatsoever in determining the pion's spectra. This is because the thermal pion's abundance is not affected by the baryon chemical potential μ_B or the strange chemical potential μ_s .

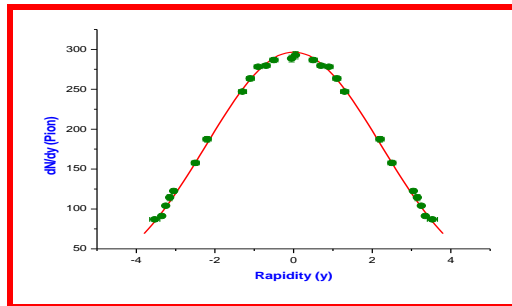


Figure (8): Rapidity spectra of pion flow.

In our analysis we have applied the criteria of exact strangeness conservation. It is done in a way such that the net strangeness is zero not only on the overall basis but also in every fireball separately. This is essential because as the rapidity of the fireballs formed increases along the rapidity axis the baryon chemical potential (μ_B) also increases. Hence the required value of the strange chemical potential (μ_s) varies accordingly for each fireball for a given value of temperature T ($= 177.0$ MeV here). Consequently the value of the strange chemical potential (μ_s) will vary with y_{FB} .

In figure (9) we have shown this by plotting the variation of the μ_s with y_{FB} . It is seen to first rise smoothly with y_{FB} reaching a maximum value of about 50 MeV at around $y_{FB} \sim 3.5$ and then drops rapidly to very small values as $y_{FB} \sim 5$ and beyond this will become negative.

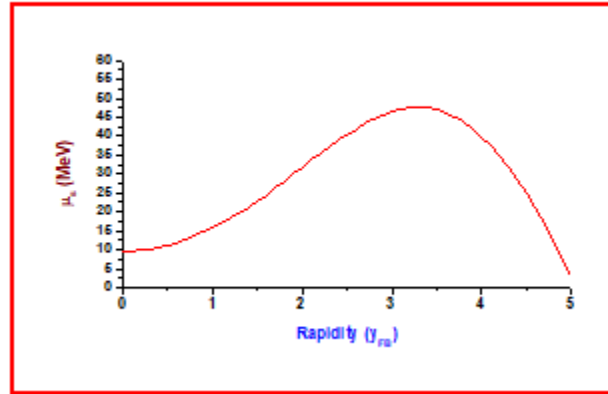


Figure (9): The variation of the μ_s with y_{FB} for $T = 175.0$ MeV.

Summarize and Conclusion:

The above results, we use an extended thermal model, where formation of several fireballs (or regions) moving with increasing rapidity (y_{FB}) along the rapidity axis is assumed. The final state hadrons are assumed to be emitted from these fireball regions. A Gaussian profile in y_{FB} is used to weigh the contributions of these regions to the final state emitted hadron's population. A quadratic profile in y_{FB} is used to fix the baryon chemical potentials of these fireballs (regions). We find that it is possible to explain not only the net proton, \bar{p}/p and pion flow but also the individual proton, antiproton, Kaon, antiKaon. It is interesting to find that the model can successfully explain the strange sector data quite well, measured in the same experiment by the BRAHMS collaboration. This is achieved by using *single* set of the model parameters.

Though for the particles mentioned above we get satisfactory rapidity distribution spectra. However the ratio K^*/K is over predicted and we also don't get a satisfactory result for \bar{K}/K and K/π ratio. Therefore it is worthwhile to attempt to explain these. Although the temperature $T=175$ MeV has good agreement with some other theoretical calculation moreover we believe that

the failure to explain the above mentioned discrepancies may lead us to a value of T which could be different for different hadronic species.

Bibliography:

- [1] E. Kornaset *et al.* NA 49 Collaboration, Eur. Phys. J. **C49** (2007) 293.
- [2] F. Becattini *et al.* arXiv : 0709.2599v1 [hep-ph].
- [3] Fu-Hu Liu *et al.*, Europhysics Letters **81** (2008) 22001.
- [4] J. Cleymans, J. Phys **G35** (2008) 1.
- [5] J. Cleymans *et al.* arXiv : 0712.2463v4 [hep-ph] 2008.
- [6] G.J. Alner *et al.* Z. Phys. **C33** (1986) 1.
- [7] I.G. Bearden *et al.*, BRAHMS Collaboration, Phys. Rev. Lett. **93**(2004)102301.
- [8] L.A. Stiles and M. Murray, nucl-ex/0601039.
- [9] B. Biedroń and W. Broniowski, Phys. Rev **C75** (2007)054905.
- [10] Fu-Hu Liu *et al.*, Europhys. Lett. **81** (2008) 22001.
- [11] Fu-Hu Liu *et al.*, Phys. Rev **C69** (2004) 034905.
- [12] Fu-Hu Liu, Phys. Rev. **C66** (2002) 047902.
- [13] Fu-Hu Liu, Phys. Lett. **B583** (2004) 68.
- [14] F. Becattini and J. Cleymans, J. Phys. **G34** (2007) S959.
- [15] F. Becattini *et al.*, Proceedings of Science, CPOD07 (2007) 012,
- [16] W. Broniowski and B. Biedroń J. Phys. **G35**(2008)044018, arXiv:0709.0126.
- [17] J. Cleymans *et al.* Phys. Rev. **C75** (2006) 034905.
- [18] J.D. Bjorken, Phys. Rev. **D27** (1983) 140.
- [19] J. adamset *et al.*, Phys. Rev. Lett. **98** (2007) 062301.